Altered MicroRNA Expression Confined to Specific Epithelial Cell Subpopulations in Breast Cancer

Lorenzo F. Sempere,[1] Mette Christensen,[4] Asli Silahtaroglu,[4] Mads Bak,[4] Catherine V. Heath,[1] Gary Schwartz,[5] Wendy Wells,[2] Sakari Kauppinen,[4,6] and Charles N. Cole[1,3]

Departments of [1]Biochemistry, [2]Pathology, and [3]Genetics, Dartmouth Medical School, Hanover, New Hampshire; [4]Wilhelm Johannsen Centre for Functional Genome Research, Department of Cellular and Molecular Medicine, University of Copenhagen, Copenhagen, Denmark; [5]Department of Medicine, Dartmouth-Hitchcock Medical Center, Lebanon, New Hampshire; and [6]Santaris Pharma, Hørsholm, Denmark

Abstract

MicroRNAs (miRNAs) are a new class of short noncoding regulatory RNAs (18–25 nucleotides) that are involved in diverse developmental and pathologic processes. Altered miRNA expression has been associated with several types of human cancer. However, most studies did not establish whether miRNA expression changes occurred within cells undergoing malignant transformation. To obtain insight into miRNA deregulation in breast cancer, we implemented an *in situ* hybridization (ISH) method to reveal the spatial distribution of miRNA expression in archived formalin-fixed, paraffin-embedded specimens representing normal and tumor tissue from >100 patient cases. Here, we report that expression of miR-145 and miR-205 was restricted to the myoepithelial/basal cell compartment of normal mammary ducts and lobules, whereas their accumulation was reduced or completely eliminated in matching tumor specimens. Conversely, expression of other miRNAs was detected at varying levels predominantly within luminal epithelial cells in normal tissue; expression of miR-21 was frequently increased, whereas that of let-7a was decreased in malignant cells. We also analyzed the association of miRNA expression with that of epithelial markers; prognostic indicators such as estrogen receptor, progesterone receptor, and HER2; as well as clinical outcome data. This ISH approach provides a more direct and informative assessment of how altered miRNA expression contributes to breast carcinogenesis compared with miRNA expression profiling in gross tissue biopsies. Most significantly, early manifestation of altered miR-145 expression in atypical hyperplasia and carcinoma *in situ* lesions suggests that this miRNA may have a potential clinical application as a novel biomarker for early detection. [Cancer Res 2007;67(24):11612–20]

Introduction

MicroRNAs (miRNA) are a recently discovered class of short noncoding RNA genes that act posttranscriptionally as negative regulators of gene expression (1, 2). A large body of research shows that animal miRNAs play fundamental roles in many biological processes, including cell growth and apoptosis, hematopoietic lineage differentiation, insulin secretion, brain morphogenesis, and muscle cell proliferation and differentiation (3). The biologically active or mature miRNA is released after sequential enzymatic cleavage of a pri-pre-miRNA molecule. First, a long, primary 5′-capped, and 3′-polyadenylated transcript is cleaved in the nucleus by Drosha and associated proteins of the microprocessor complex to release a canonical 70-nucleotide precursor hairpin, which is exported to the cytoplasm via the exportin-5 pathway where it is further cleaved by a Dicer/Argonaute multiprotein complex to yield the mature miRNA (4). Binding of the mature ~18- to 25-nucleotide-long miRNA, in association with the Dicer/Argonaute complex, to partially complementary sites in the 3′-untranslated region of target mRNAs triggers translational down-regulation and/or increased degradation of the target mRNA (5).

About 1,000 miRNA genes are thought to be encoded in the human genome (6, 7). Although it is still difficult to identify accurately individual miRNA/target interactions (8), computational predictions of miRNA target genes indicate that as many as one third of all human protein-encoding genes may be regulated by miRNAs (9). This suggests that miRNAs could be involved in a wide variety of human diseases, including cancer. Indeed, as a result of intense research within the last 5 years, miRNA-mediated regulation of tumorigenesis is emerging as a new paradigm in the field of cancer biology (10, 11). The first association between miRNAs and cancer was the detection of frequent chromosomal deletion and/or expression down-regulation of miR-15a and miR16-1 in B-cell chronic lymphocytic leukemia (12). Subsequently, a unique expression signature affecting 13 miRNA genes has been linked to prognosis and progression of this disease (13). Specific subsets of miRNAs have also been shown to be deregulated in solid tumors of the colon, lung, pancreas, and other organs. For example, reduced expression of miR-143 and miR-145 is associated with the adenomatous and cancer stages of colorectal neoplasia (14), whereas low expression of let-7 and high expression of miR-155 correlate with poor outcome for patients with lung adenocarcinoma (15). It has also been reported that these miRNA signatures may be a more robust tool than expression patterns of protein-encoding genes for distinguishing normal from tumor tissues (16, 17). Importantly, miRNA genes associated with these cancer signatures fulfill the criteria to be considered as oncogenes or tumor suppressor genes. Overexpression of the polycistronic miRNA cluster miR-17–miR-92 accelerates tumor development in a c-Myc–induced mouse model of B-cell lymphoma (18), indicating that one or more miRNAs in this cluster function as an oncogene. In contrast, miR-15 and miR-16 function as tumor suppressors to modulate the expression

Note: Supplementary data for this article are available at Cancer Research Online (http://cancerres.aacrjournals.org/).

Current address for L.F. Sempere: Department of Medicine, Dartmouth-Hitchcock Medical Center, Lebanon, New Hampshire.

W. Wells, S. Kauppinen, and C.N. Cole contributed equally to this work.

Requests for reprints: Lorenzo F. Sempere, Department of Medicine, Dartmouth-Hitchcock Medical Center, Lebanon, NH 03766. Phone: 603-653-9936; Fax: 603-653-9952; E-mail: Lorenzo.F.Sempere@dartmouth.edu.

doi:10.1158/0008-5472.CAN-07-5019

of antiapoptotic gene *Bcl-2* in MEG-01 leukemic cell line (19), and let-7, a founding member of the miRNA gene family, acts in a similar fashion to modulate the expression of proto-oncogenic N-Ras and K-Ras in lung adenocarcinoma cells (20). Thus, profiling of miRNAs in human cancer has generated great interest not only because miRNAs could serve as useful biomarkers for early detection, diagnosis, and/or prognosis but also because they could shed light onto the molecular mechanisms of the tumorigenic process and have high potential as novel targets for therapeutic intervention using synthetic oligonucleotide technologies.

Breast carcinoma, which is the second most prevalent cancer in women, is a complex, inadequately understood, and often fatal disease when not detected at early stages. Microarray analyses of mRNAs indicate that breast tumors can be grouped into four major subtypes (luminal A, luminal B, HER2 overexpressing, and basal) that differ with respect to their patterns of gene expression, phenotypes, prognosis, and susceptibility to specific treatments (21, 22). Microarray data also indicate the involvement of distinct subpopulations of epithelial cells among tumor subtypes: cells with myoepithelial/basal characteristics contribute almost exclusively to the basal subtype. The gene expression subtypes closely correspond to a more traditional classification based on the status of estrogen receptor (ER), progesterone receptor (PR), and human epidermal growth factor receptor-like 2 (HER2/neu) because targeted drugs have been developed to block their signaling pathways (23). ER^+ and/or PR^+ and $HER2^-$ tumors (luminal A) are more likely to respond to antiestrogens and aromatase inhibitors, ER^+ and/or PR^+ and $HER2^+$ ($\sim$30% of luminal B cases) and $ER^-PR^-HER2^+$ (HER2 overexpressing) respond to trastuzumab, whereas $ER^-PR^-HER2^-$ cases (basal) do not respond to any of these targeted treatments but seem to respond more favorably than other subtypes to neoadjuvant chemotherapy regimens (24, 25).

Because multiple miRNAs are usually associated with a given cancer signature, determining whether the observed miRNA expression changes occur within malignant cells rather than involved stroma, infiltrating lymphocytes, and/or vasculature is essential to select appropriate miRNA(s) for further clinical studies and functional analysis. This is especially important in solid tumors such as breast carcinoma because heterogeneity of cell types between normal and tumor tissue and among tumors may confound the nature of altered miRNA expression. In this study, we determined the miRNA expression profiles in a collection of extensively studied breast cell lines and in normal and tumor breast tissue specimens using locked nucleic acid (LNA) microarrays (26–28). Then, we implemented an *in situ* hybridization (ISH) method to determine the cell type specificity of miRNA expression in formalin-fixed, paraffin-embedded (FFPE) tissue specimens. We identified several miRNAs whose expression is altered within distinct subpopulations of mammary epithelial cells. miR-145 and miR-205 expression was restricted to myoepithelial cells in normal epithelial structures, whereas their expression was reduced or completely eliminated in matching tumor specimens. Conversely, expression of let-7a, miR-21, miR-141, and miR-214 was detected at varying levels predominantly within luminal epithelial cells in normal tissue. miR-21 expression was frequently increased, whereas let-7a expression was decreased in malignant cells, and expression of miR-141 and miR-214 exhibited a more complex pattern. Together, our results provide a more profound understanding of the etiologic relevance of altered miRNA expression in breast cancer and suggest that each of these cell type–confined miRNAs may operate through distinct mechanisms to affect breast carcinogenesis. The potential clinical applications of these findings are also discussed.

Materials and Methods

Cell lines and culture. BT-474, MCF7, MDA-MB-231, MDA-MB-453, and MDA-MB-468 were purchased from the American Type Culture Collection. BT-549, HS578T, NCI/ADR-RES, and MDA-MB-435 were obtained as frozen pellets and are components of the NCI-60 cell panel.[7] MCF10A, MCF10A[Myc], MCF10A[Δp53], SK-BR-3, and immortalized mammary epithelial cells (IMEC) were obtained from different colleagues. BT-474, MCF7, MDA-MB-231, MDA-MB-453, MDA-MB-468, and SK-BR-3 were cultured in DMEM/F12 (Cellgro) supplemented with 10% fetal bovine serum, 2 mmol/L L-glutamine, penicillin, and streptomycin; MCF10A, MCF10A[Myc], and MCF10A[Δp53] were cultured in the above medium with the addition of 8 μg/mL insulin, 20 ng/mL human epidermal growth factor (EGF), and 500 ng/mL hydrocortisone. IMECs were cultured in mammary epithelial growth medium (Clonetics) supplemented with 0.5 μg/mL puromycin, penicillin, and streptomycin.

Tissue specimens and generation of the tissue microarray. The Tissue Bank at Dartmouth-Hitchcock Medical Center maintains frozen tissue and a series of FFPE tissue blocks of patients with breast cancer diagnoses. Information on tumor size, nodal status, histologic grade, hormone receptor status, HER2 amplification status, date of diagnosis, date of recurrence, and date of death was collected and anonymized in a secure database. For generation of the tissue microarray (TMA), patient cases were selected based solely on ER/PR/HER2 status: 25 $ER^+PR^+HER2^-$, 25 $ER^+PR^-HER2^-$, 25 $ER^{+/-}PR^{+/-}HER2^+$, and 25 $ER^-PR^-HER2^-$. The ER and PR expression was determined by immunohistochemistry, and cases with equivocal immunostaining (1–15% tumor nuclei positive) were excluded. HER2 amplification was confirmed by Food and Drug Administration–approved PathVysion FISH Assay (Abbott-Vysis). All FFPE blocks were reviewed and tissue cores were selected by a board-certified pathologist (W.W.). A core cylinder with a diameter of 0.6 mm was punched and deposited into a recipient paraffin block using a manual arrayer (Beecher Instruments, Inc.).

Microarray analysis. The LNA-modified oligonucleotide probe set for all annotated miRNAs from mouse (*Mus musculus*) and human (*Homo sapiens*) in the miRBase Release 7.1 was purchased from Exiqon and used to fabricate the LNA microarrays (see Supplementary Data for details). Total RNA extracted from breast cell lines or frozen tissue specimens was extracted with Trizol reagent (Invitrogen) and 3′-end labeled using T4 RNA ligase to couple Cy3- or Cy5-labeled RNA linkers (29, 30). Labeled RNA was hybridized to LNA microarrays overnight at 65°C in a hybridization mixture containing 4× SSC (1× SSC solution is 150 mmol/L sodium chloride and 15 mmol/L sodium citrate), 0.1% SDS, 1 μg/μL herring sperm DNA, and 38% formamide. After hybridization, slides were washed thrice in 2× SSC and 0.025% SDS at 65°C followed by thrice in 0.8× SSC and finally thrice in 0.4× SSC at room temperature. The microarrays were scanned using an arrayWoRx scanner (Applied Precision) according to the manufacturer's recommendations. The scanned images were imported into The Institute for Genomic Research Spotfinder version 3.1 (31) for the extraction of mean spot intensities and median local background intensities, excluding spots with intensities below median local background + 4 SDs. Background-correlated intensities were normalized using variance-stabilizing normalization package version 1.8.0 (32) for R.[8] Probes displaying a coefficient of variance >100% were excluded from further data analysis. Statistical comparisons were carried out using The Institute for Genomic Research MultiExperiment Viewer (31).

Northern blot analysis. Total RNA from each breast cell line or frozen tissue specimen (5 μg/lane) was used to perform Northern blots as described by Sempere et al. (33). miRNA and snoRNA U6 antisense StarFire (Integrated DNA Technologies) radioactively labeled probes were prepared

[7] http://dtp.nci.nih.gov/
[8] http://www.r-project.org

by incorporation of 6,000 Ci/mmol [α-^{32}P]dATP as recommended by the vendor. Radioactive signals originating from the miRNA bands were divided by the signal of background membrane squares of the same size. This quotient represents fold expression over background. Values were also corrected for loading differences based on the U6 signal. Cluster analysis was performed using CIMminer.[9]

Detection of miRNAs by ISH in FFPE sections. Sections (4 μm) of archived paraffin-embedded specimens were deparaffinized in xylenes and then rehydrated through an ethanol dilution series (from 100% to 25%). Slides were submerged in diethyl pyrocarbonate–treated water and subjected to proteinase K digestion (5–10 μg/mL) and 0.2% glycine treatment, refixed in 4% paraformaldehyde, and treated with acetylation solution [66 mmol/L HCl, 0.66% (v/v) acetic anhydride, and 1.5% (v/v) triethanolamine]; slides were rinsed thrice with 1× PBS between treatments. Slides were prehybridized in hybridization solution (50% formamide, 5× SSC, 500 μg/mL yeast tRNA, and 1× Denhardt's solution) at 50°C for 30 min. Then, 5 to 10 pmol of FITC-labeled, LNA-modified DNA probe (Exiqon or Integrated DNA Technologies) complementary to a given miRNA were added to the 150 μL of hybridization solution and hybridized for 2 h at a temperature of 20°C to 25°C below the calculated T_m of the LNA probe. After washes in SSC at increasing stringency (from 2× to 0.2×) at the same temperature as of the hybridization, a tyramide signal amplification reaction was carried out using the GenPoint Fluorescein kit (DakoCytomation) following the vendor's recommendations. Finally, slides were mounted with Prolong Gold solution (Invitrogen). Signals were visually quantified by L.F. Sempere using quick score system from 0 to 5, combining intensity of signal and percentage of positive cells (signal: 0 = no signal, 1 = weak signal, 2 = intermediate signal, 3 = strong signal; percentage: 0 = 0%, 1 = <30%, 2 = >30%). Tissue sections were blindly examined by a second individual (W.W. and/or A.S.) and this yielded a good agreement with the initial quantifications.

Results

Expression profiling of miRNAs in normal and tumor breast tissue. To identify miRNAs differentially expressed in breast cancer, we used LNA microarrays to profile miRNA expression in normal and tumor breast specimens. Our spotted LNA oligonucleotide arrays contain capture probes for all annotated human miRNAs in the miRNA database miRBase Release 7.1 (28, 34). Experiments were conducted with total RNA isolated from four matched normal/tumor specimens that were $ER^+PR^+HER2^-$ as well as two tumor $ER^-PR^-HER2^+$ and four tumor $ER^-PR^-HER2^-$ specimens. Microarray expression profiling revealed >20 miRNAs that showed distinct expression patterns. Most commonly, miRNAs were expressed at higher levels in tumor specimens (Fig. 1*A*); miR-21 was consistently up-regulated across tumor specimens ($P = 0.03$, Student's t test), whereas other miRNAs (miR-141, miR-200b, miR-200c, miR-214, miR-221, and miR-222) exhibited a more irregular pattern, being highly expressed in some and completely absent in other specimens. Interestingly, miR-205 was highly expressed in two of the four $ER^-PR^-HER2^-$ specimens, suggesting perhaps an association of miR-205 expression with this aggressive tumor subtype or a distinct subset of cases within this tumor subtype (see below for a detailed explanation). Only two miRNAs were identified that showed a consistent pattern of high expression in normal specimens and low expression in tumor specimens: miR-145 ($P = 0.003$) and miR-451 ($P = 0.018$). To confirm these findings, we examined expression of a subset of miRNAs by Northern blot analysis in 11 normal and 25 tumor specimens that included all available specimens used for LNA microarray profiling as well as additional specimens (Fig. 1*B*). Overall, results obtained by LNA microarray and Northern blot analyses were concordant. We observed minor differences between these two techniques that relate to the magnitude of expression changes between normal and tumor specimens but not the direction of these changes.

miRNA expression can distinguish breast cell lines based on their malignancy status and cellular origin. Because differences in miRNA levels detected among normal and tumor breast specimens may be due simply to tissue heterogeneity and/or unequal contribution of different cell types to the tumor mass (e.g., adipocytes versus epithelia), we set out to determine whether observed miRNA expression changes occur within epithelial cells undergoing malignant transformation. LNA microarrays and Northern blot analyses were used to measure miRNA levels in a collection of breast epithelial cell lines (BCL): two are nontumorigenic (IMECs and MCF10A), whereas the rest are tumorigenic BCLs isolated from tumors or genetically transformed in the laboratory. miRNAs showed a variety of expression patterns in these BCLs (Fig. 1; Supplementary Figs. S1 and S2). Some were highly restricted to one or few BCLs (miR-145 and miR-205), whereas others were more widely expressed (let-7, miR-92, and miR-181; Fig. 1). Induction of miR-145 expression in MCF10A[Myc] does not seem to be a direct consequence of c-Myc activation because IMECs transformed with c-Myc do not overexpress miR-145 (data not shown). Interestingly, we observed several miRNAs whose expression was elevated in tumorigenic cell lines compared with nontumorigenic ones (miR-21, miR-23, and miR-191), whereas only miR-205 was consistently down-regulated in tumorigenic cell lines (Fig. 1*C* and *D*). miR-451 expression was not detected in any of the cell lines studied, suggesting that expression changes observed in RNA extracted from gross tissue specimens correspond to a cell type of nonepithelial origin.

Eleven BCLs in our panel can be grouped in basal and luminal categories based on transcriptional profiling and/or cytokeratin expression (35, 36). Expression of some miRNAs was restricted to BCLs within each group (Fig. 1*C*). miR-141–mir200c (tightly linked on chromosome 12) and miR-183 showed a very similar pattern that was opposite to that of mir-221–miR-222 (tightly linked on chromosome X). These differences were sufficient to distinguish luminal from basal BCLs. The expression of these miRNAs may reflect a common cell type origin or common evolution of these tumor cells.

MCF7 and T-47D are ER^+ cell lines and respond to estrogen activation, whereas BT-474, MDA-MB-453, and SK-BR-3 are known to overexpress the HER2. Treatment of responsive cells with fulvestrant (antagonist competitive ligand of estrogen) or with trastuzumab (humanized antibody against the ectodomain of HER2) did not affect expression of examined miRNAs (data not shown). These findings are consistent with the fact that we do not observe miRNA expression patterns that correlate exclusively with ER or HER2 status.

Detection of miRNA expression by ISH analysis in archived breast tissue specimens. Expression patterns of some miRNAs in BCLs may be a consequence of the specific characteristics of the subpopulation of cells isolated to establish the BCL and/or prolonged growth in culture without stromal interaction. To circumvent these potential limitations, we implemented an ISH method to visualize miRNA expression at higher spatial resolution. The detection of mature miRNAs by ISH is technically challenging because of their small size. LNAs are a class of bicyclic high-affinity

[9] http://discover.nci.nih.gov/nature2000/tools/cimmaker.jsp

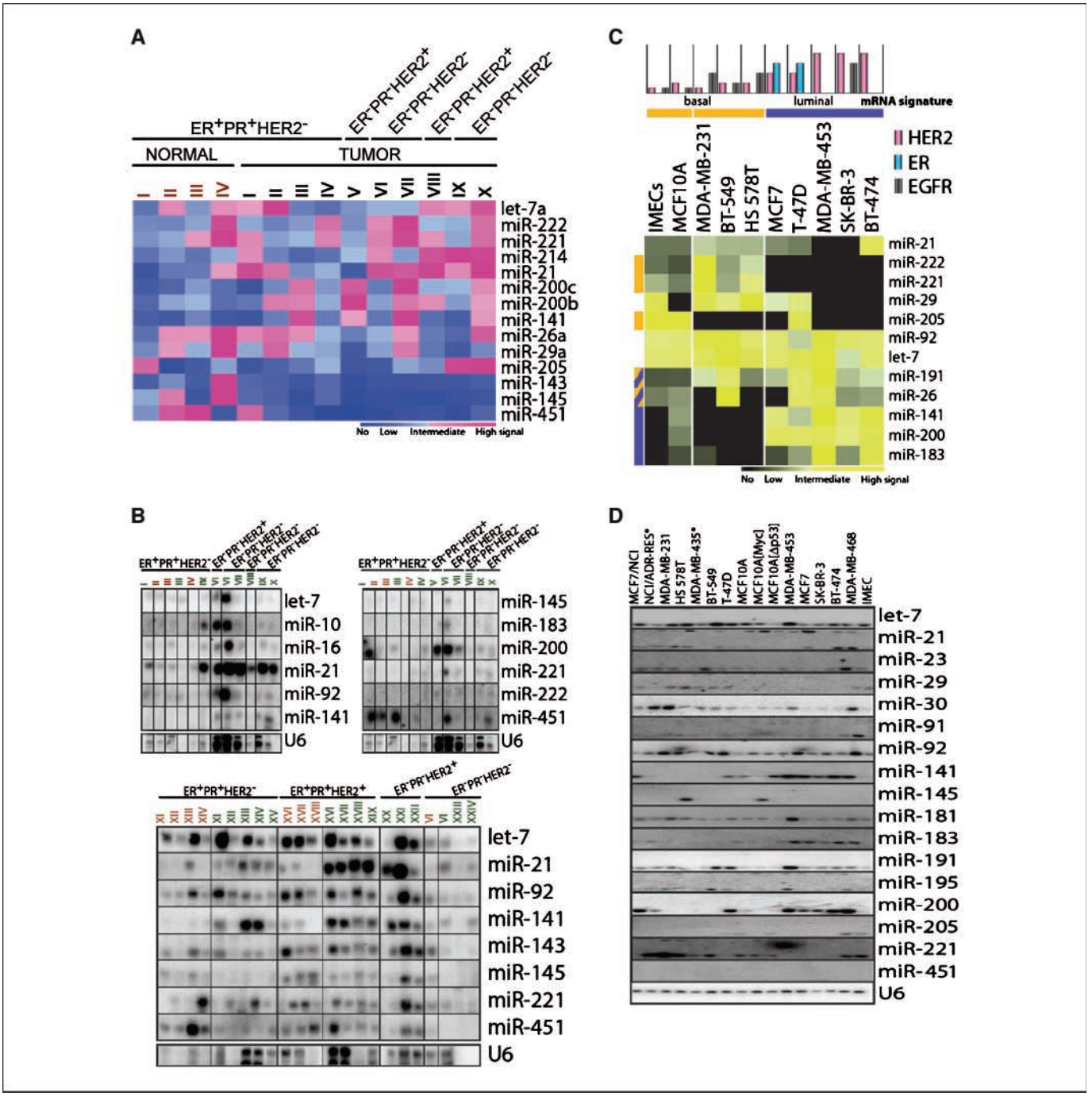

Figure 1. Expression profiling of miRNAs in breast cancer cases and cell lines. Total RNA was extracted from frozen normal (*red*) and tumor (*green*) breast tissue specimens and breast cell lines. *A,* colored heatmap displays mean values of miRNA expression from two to three independent normalized array data sets. *B,* Northern blots of selected miRNAs in the same set of patient cases as used for LNA microarray experiments (*top*) as well as in an additional set of patients (*bottom*) are displayed. Patient cases are clustered by normal and tumor classes, and within each class, they are grouped by their common ER/PR/HER2 status. *C,* miRNA levels were quantified from radioactive signals of Northern blots displayed in *D*. Signal values were corrected for loading (using the U6 signal) and normalized using relative values from 0 (no signal; *black*) to 100 (highest value; *bright yellow*). BCLs are grouped by their common gene expression signatures (35, 36). The levels of ER, EGFR, and HER2 are those that have been reported in the literature (35, 36). *D,* Northern blots of selected miRNAs in a panel of commonly used BCLs. MCF10A and IMECs are the only nontumorigenic BCLs in this panel. Two different MCF7 preparations were used: one cultured in our laboratory and the other obtained as a nonviable frozen cell pellet as part of the NCI-60 cell panel (*MCF7/NCI*). *Asterisk,* the breast origin of MDA-MB-435 and NCI/ADR-RES has recently been questioned (48, 49) and they were excluded from data analysis.

RNA analogues in which the furanose ring in the sugar-phosphate backbone is chemically locked in a conformation mimicking the North-type (C3′-endo) conformation of RNA (26, 27). This results in an unprecedented hybridization affinity of LNA toward complementary single-stranded RNA molecules. Recently, LNA-modified DNA probes have been used to determine the spatiotemporal expression patterns of miRNAs in zebrafish and mouse embryos by whole-mount ISH (30, 37) as well as in archived FFPE sections of

brain tissue (38). Here, we used 5′ FITC-labeled, LNA-modified DNA oligonucleotide probes complementary to the entire mature sequence of a subset of selected miRNAs. Following hybridization of the LNA probes to the FFPE sections, a tyramide signal amplification reaction was carried out (39) using horseradish peroxidase conjugated to anti-FITC antibodies.

We generated a TMA from archived FFPE blocks of 100 breast cancer cases with detailed pathologic characterization and known clinical outcome with a follow-up period of at least 4 years (Fig. 4). These cases represent all major tumor subtypes based on the status of ER, PR, and HER2 (Fig. 4). When available, four 0.6-mm cores were used to represent each patient case: one normal, one carcinoma *in situ* (CIS), and two invasive carcinoma (ICa) cores. Expression of miRNAs and cytokeratins 14 (CK14; basal) and 19 (CK19; luminal) was determined on 4-μm sections obtained from each of the TMA blocks. We focused on miR-21, miR-141, miR-145, miR-205, miR-214, and miR-451 because they were expressed at high levels and showed substantial differences in normal versus tumor specimens and/or BCLs. We also chose to study let-7a because results from a recent study suggested that let-7a was down-regulated in breast cancer (40). We did not find a consistent pattern of expression for miR-141 and miR-214 (Figs. 2–4) that could be associated with the pathologic status of the cells or other clinical variables studied (Fig. 4; data not shown). We describe below the main findings for the other miRNAs examined.

let-7a is predominantly expressed in luminal epithelia and its expression is down-regulated in malignant cells. In normal tissue, the let-7a probe revealed an intense cytoplasmic signal in luminal epithelial cells both in ductal and lobular structures, whereas a less intense signal was commonly observed in adjacent myoepithelial cells (Fig. 2). let-7a was also detected in endothelial cells lining blood vessels and in fibroblasts (data not shown). In tumor tissue, let-7a expression was readily detectable in carcinoma cells, although frequently expression was lower than in matching normal tissue (Figs. 3 and 4; Supplementary Fig. S3). Quantification of let-7a signal indicated that decreased let-7a expression in cells of epithelial origin in CIS and ICa compared with normal was statistically significant ($n = 33$, $P = 0.005$, Wilcoxon signed-ranks test; $n = 51$, $P < 0.001$, Wilcoxon signed-ranks test, respectively). The apparent discordance between ISH and expression profiling results could be explained by the overrepresentation of epithelial cells in tumor lesions, which results in high let-7 signal detection in gross tissue biopsies. However, let-7a expression is diminished within individual cancer cells, which can be determined only by the ISH approach.

miR-21 is expressed in luminal epithelia and its expression is induced in malignant cells. In normal tissue, the miR-21 probe revealed a cytoplasmic signal only in luminal epithelial cells that ranged from a weak to strong intensity (Figs. 2 and 3), but in some cases, it was not detected at all. Occasionally, miR-21 was also detected in fibroblasts (Supplementary Fig. S3). In tumor tissue, miR-21 was frequently detected at higher levels in carcinoma cells than in matching normal tissue (Figs. 3 and 4). In some cases, miR-21 expression was also elevated in tumor-associated fibroblasts (TAF), and in a few cases, miR-21 was only detected in TAF and not in carcinoma cells (Supplementary Fig. S4). Quantification of miR-21 signal indicated that increased miR-21 expression in cells of epithelial origin in CIS and ICa compared with normal was

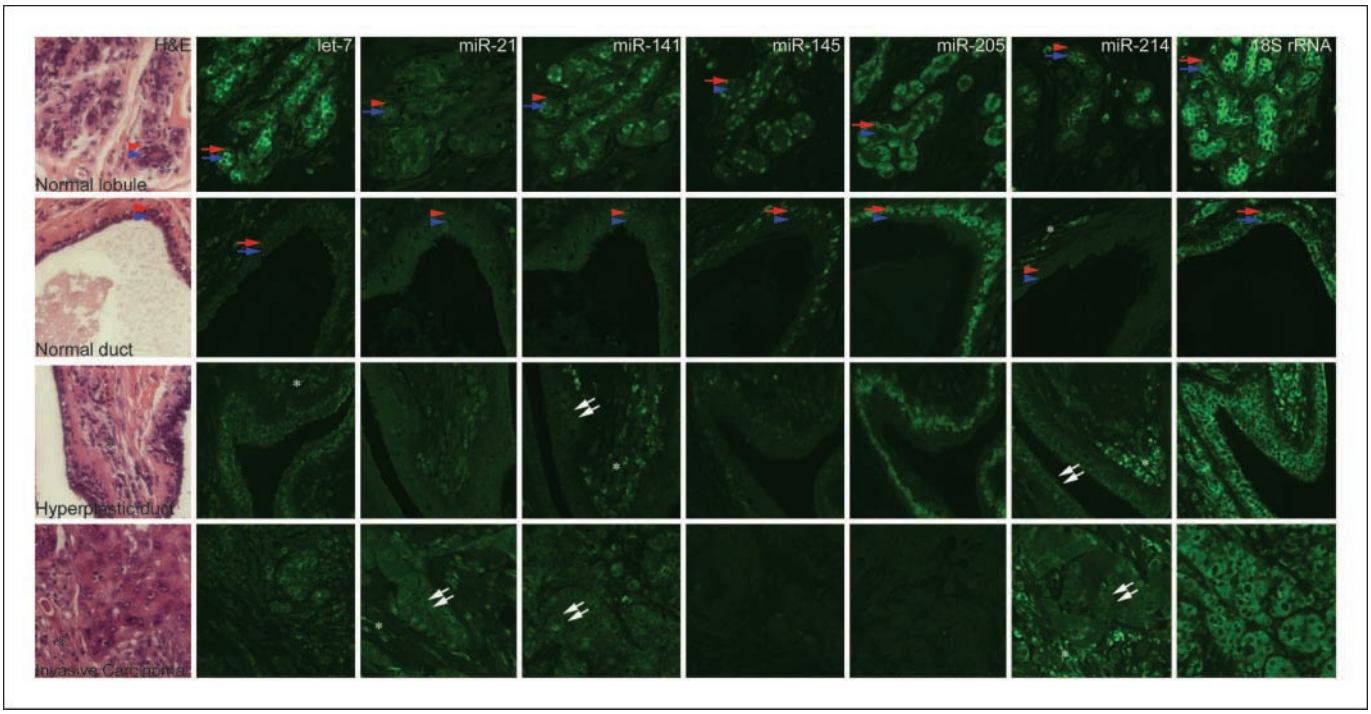

Figure 2. Expression of specific miRNAs is confined to luminal or myoepithelial cell compartments in normal breast tissue. *In situ* hybridization analyses using 5′ fluorescein-conjugated, LNA-modified DNA probes complementary to let7-a, miR-21, miR-141, miR-145, miR-205, and miR-214 and 18S rRNA (control) were performed on consecutive 4-μm sections obtained from an archived FFPE block of a $ER^+PR^+HER2^-$ patient case. An additional section was stained with H&E to reveal overall morphology. In normal lobular and ductal structures, myoepithelial (*red*) and luminal cells (*blue*) are indicated by *arrowheads*; RNA expression in these cell types is indicated with *arrows* of the corresponding color. *Bottom, white arrows,* induced miRNA expression in presumably preneoplastic cells adjacent to ICa (hyperplastic duct) and/or malignant cells (ICa). *Asterisk,* expression of some miRNAs is also detected in normal and/or TAFs.

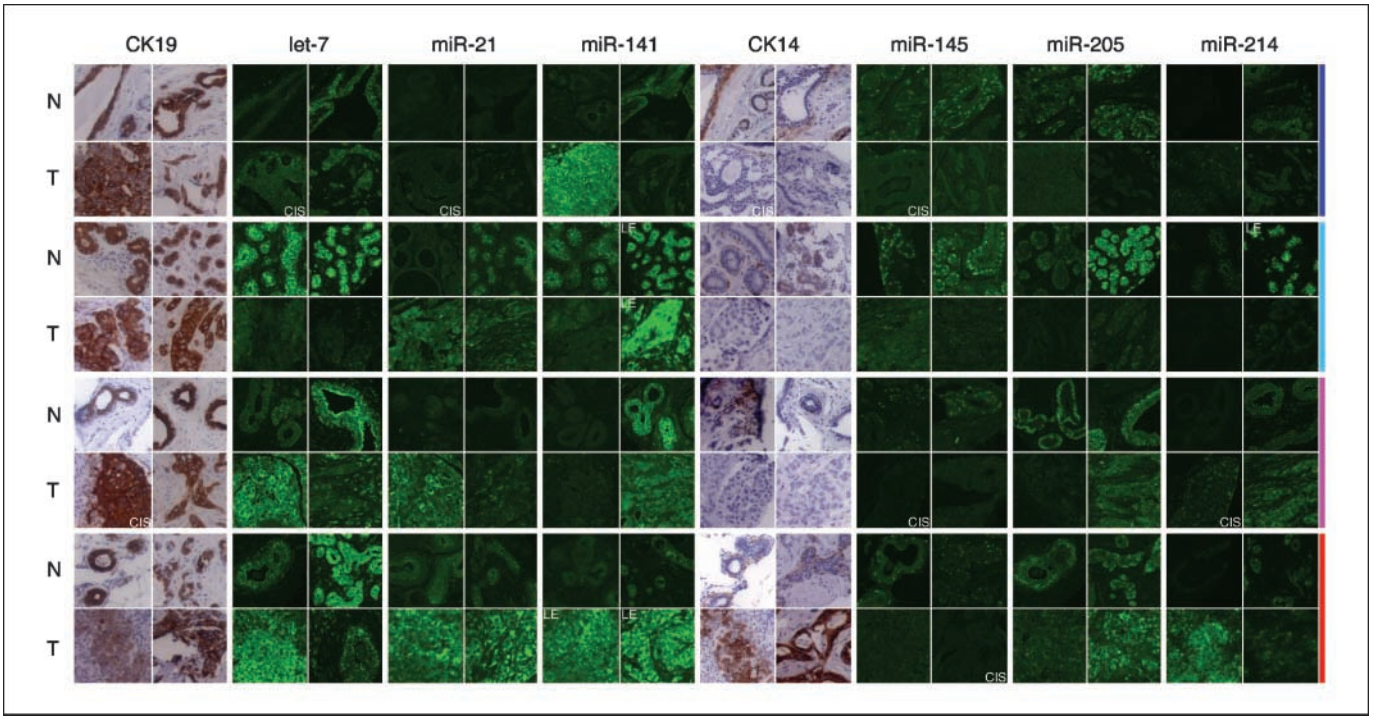

Figure 3. Altered expression of miRNAs in different tumor subtypes of breast cancer. *In situ* hybridization analyses using 5′ fluorescein-conjugated, LNA-modified DNA probes complementary to the indicated miRNA or immunohistochemical analyses of cytokeratin expression (CK19, luminal marker; CK14, basal marker) were performed on consecutive 4-μm sections obtained from archived FFPE blocks of our TMA. A field from normal (*N*) and tumor (*T*) 0.6-mm cores of two randomly selected cases representing each major tumor subtype of breast cancer is displayed: $ER^+PR^+HER2^-$ (*dark blue*), $ER^+PR^+HER2^+$ (*cyan*), $ER^-PR^-HER2^+$ (*pink*), and $ER^-PR^-HER2^-$ (*red*). Normal sections display either lobular or ductal structures; tumor sections display ICa lesions, unless indicated on individual panels to represent CIS. Immunostained sections with CK14 and CK19 antibodies were counterstained with hematoxylin to reveal nuclear morphology. *LE,* low exposure of indicated panel due to saturation of fluorescent signal, and thus, actual expression levels are higher than displayed here.

statistically significant ($n = 34$, $P = 0.04$, Wilcoxon signed-ranks test; $n = 54$, $P < 0.001$, Wilcoxon signed-ranks test, respectively), whereas no association was found with expression in TAFs.

miR-145 is expressed in myoepithelial cells and expression changes are apparent at early stages of breast cancer progression. In normal tissue, the miR-145 probe revealed a nuclear-enriched signal in myoepithelial cell layer of lobules and ducts (Figs. 2 and 3) and in smooth muscle cells within blood vessels (Supplementary Fig. S5). A noticeable decrease of miR-145 expression was observed in hyperplastic, probable preneoplastic, ducts present in some of the cases examined (Fig. 2). In tumor tissue, miR-145 expression was dramatically reduced or completely eliminated in epithelial cells within CIS ($n = 34$, $P < 0.001$, Wilcoxon signed-ranks test) and ICa lesions ($n = 51$, $P < 0.001$, Wilcoxon signed-ranks test). We also observed a reduction in miR-145 expression in smooth muscle cells within tumor-involved blood vessels (Supplementary Fig. S5). Because we did not select tissue cores to represent normal/tumor vasculature on our TMA, we cannot assess the clinical relevance of this reduced accumulation of miR-145 in our limited panel of samples.

Nuclear expression of miR-145 was consistently detected in myoepithelial cells and in smooth muscle cells of blood vessels of murine mammary gland and other organs (Supplementary Fig. S5; data not shown). We also observed miR-145 expression in the muscularis externa, muscularis mucosae, and myoepithelial cells around crypts of murine colon (Supplementary Fig. S5). Because miR-145 down-regulation has been associated with colorectal neoplasia, our result suggests the involvement of a similar miR-145–mediated process in both breast and colon cancer.

miRNAs are thought to be localized to the cytoplasm where they bind to mRNA targets and repress gene expression. Thus, nuclear localization of miR-145 suggests a novel regulatory mechanism for this miRNA. This is not an unprecedented observation because a hexanucleotide element at the 3′-end of miR-29b has been found to be sufficient to direct miRNA/small interfering RNA nuclear import (41). Although the 3′-end of miR-145 has no homology to the miR-29b sequence, perhaps miR-145 contains a distinct import element.

miR-205 is exclusively expressed in normal myoepithelial cells and its expression is down-regulated in malignant cells. In normal tissue, the miR-205 probe revealed an intense cytoplasm-enriched signal exclusively within myoepithelial cells in lobules and ducts (Fig. 2; Supplementary Fig. S6). Unlike miR-145, the offset of miR-205 expression occurs after the atypical hyperplasia stage. miR-205 expression changes are statistically significant at the CIS ($n = 31$, $P < 0.001$, Wilcoxon signed-ranks test) and ICa stages ($n = 51$, $P < 0.001$, Wilcoxon signed-ranks test) compared with normal.

Because transformed cells within the myoepithelial/basal compartment are thought to be involved mainly in cases classified as basal tumor subtype ($ER^-PR^-HER2^-$; refs. 21, 23, 24, 42), lack of miR-205 expression in other tumor subtypes may simply reflect the origination of these tumor cells from a nonmyoepithelial cell subpopulation. To test whether miR-205 is altered in malignant cells with myoepithelial characteristics, we performed immunohistochemical assays to detect expression of the basal epithelial marker CK14 for all cases included in our TMA blocks. Positive (intense and diffused) CK14 staining was only observed in $ER^-PR^-HER2^-$ cases (Figs. 3 and 4), consistent with previous reports (43, 44). With the exception of a minority of $ER^-PR^-HER2^-$

cases (2 of 20), miR-205 expression was detected at lower levels in $CK14^+$ carcinoma cells compared with normal myoepithelial cells, suggesting that reduction of miR-205 expression is associated with tumor progression. Dichotomization of $ER^-PR^-HER2^-$ cases by low (score 0 to 3) and high (score 4 to 5) miR-205 expression separates cases with a favorable clinical outcome from those with a poor outcome (Fig. 4; Supplementary Fig. S6). One of 5 cases with high miR-205 expression relapsed, whereas 6 of 15 with low expression relapsed and succumbed to the disease within 2 years of recurrence. This observed trend suggests that miR-205 may serve as a predictor of disease outcome in $ER^-PR^-HER2^-$ cases, although a much larger sample size is needed to assess the clinical relevance of this correlation.

miR-451 is exclusively expressed in erythrocytes. miR-451 was detected exclusively in mature enucleated RBCs both in human breast and murine heart and in other tissues (Supplementary Fig. S7). This result is consistent with lack of miR-451 expression in any of the BCLs examined and with a recent report suggesting a role for miR-451 in erythroid maturation (45). The apparent down-regulation of miR-451 in tumor specimens compared with normal in our microarray experiments may simply reflect a different architecture of the tumor-involved vasculature, which poorly irrigates the tumor mass. This further underscores the importance of assessing miRNA expression by ISH detection in FFPE sections to confirm results of miRNA expression profiling in gross tissue biopsies.

Discussion

Breast cancer is diagnosed in >200,000 women in the United States every year. Four major breast tumor subtypes have been identified based on gene expression profiling, which in general correspond to a specific status of ER, PR, and HER2 (23). In this study, we report a miRNA signature within distinct subpopulations of luminal and myoepithelial cells that reliably separates normal from tumor specimens. In our limited cohort of cases, we do not observe a clear association between changes of miRNA expression and ER/PR/HER2 status, although there is a

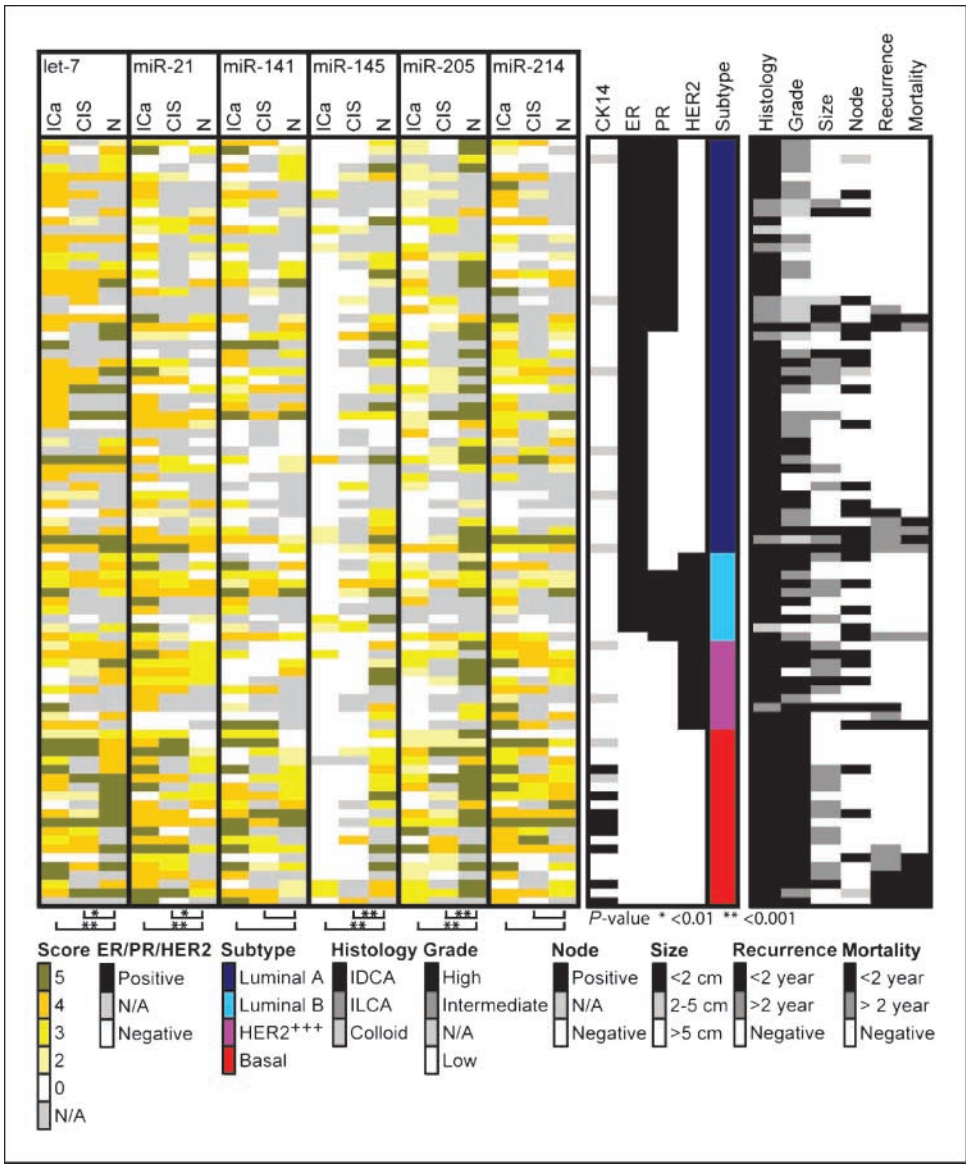

Figure 4. Correlation of miRNA expression with pathologic and clinical outcome data in a cohort of 87 patient cases. On the left, the heatmap displays miRNA expression in epithelial cells within normal, CIS, and ICa tissue using a scoring system from no signal = 0 to diffuse and intense signal = 5 (see Materials and Methods). Interpretable results were obtained from 87 of these 100 cases included in the TMA. In some cases, not enough material was present for scoring miRNA expression and/or other variables (*N/A*). The status of CK14 and ER/PR/HER2, histologic characteristics, and outcome data are shown. *IDCA,* invasive ductal carcinoma; *ILCA,* invasive ductal carcinoma. Patient cases are sorted by ER/PR/HER2 status and, within each group, by their disease outcome (*Mortality*), which is expressed as elapsed time between detection of disease recurrence and death. The corresponding gene expression subtype to each ER/PR/HER2 status is shown as reference only because microarray analyses were not performed on these specimens.

trend for higher miR-21 expression in ER^- cases ($n = 81$, $P = 0.012$, Mann-Whitney test). Indeed, we believe that individual miRNAs identified in this signature have the potential to serve as new independent biomarkers for management of different pathologic subtypes of breast cancer, as we briefly discuss below.

Our initial expression profiling experiments identified several miRNAs that were differentially expressed between normal and tumor tissue specimens and among breast cell lines (Fig. 1). A subset of these miRNAs was further studied by LNA-ISH in a cohort of >100 patient cases (TMA cases plus individual cases), about half of which had matching normal and tumor tissue, representing different ER/PR/HER2 subtypes, tumor grades, and stages of the disease (Fig. 4). We find that let-7a, miR-21, miR-141, and miR-214 are preferentially expressed in luminal cells, whereas miR-145 and miR-205 are expressed in myoepithelial cells (Figs. 2 and 3). The most significant changes in ICas are the frequent and dramatic decrease of miR-145 and miR-205 expression and elevation of miR-21 expression. Whereas no detection of miR-145 and miR-205 expression in $ER^+PR^{+/-}HER2^-$ and $ER^-PR^-HER2^+$ cases may simply reflect the nonmyoepithelial origin of their carcinoma cells, no/low expression in $CK14^+$ malignant cells suggests that miR-145 and miR-205 down-regulation is a consequence of disease progression in $ER^-PR^-HER2^-$ cases. Alternatively, malignant cells might originate from a myoepithelial cell subpopulations with initial low expression of these miRNAs or from nonmyoepithelial cells with plasticity to acquire myoepithelial/basal cell characteristics. Overall, our results are in good agreement with a recent study that profiled miRNA expression using total RNA extracted from breast biopsies and found miR-145 as the most significantly down-regulated and miR-21 as the most significantly up-regulated miRNAs (40). This recurrent identification suggests that changes in the levels of these miRNAs may have important functional consequences during breast tumorigenesis. Of note, the confined expression of these miRNAs to distinct subpopulations of epithelial cells and their distinct intracellular localizations suggests that each miRNA may affect the tumorigenic process through different mechanisms.

Altered expression of miR-145 and miR-205 within myoepithelial/basal exhibits different dynamics and patterns during disease progression. Decrease of miR-145 expression is already apparent in hyperplastic (probable preneoplastic) ducts when myoepithelial architecture is mildly compromised. Further decrease of miR-145 in CIS lesions is reminiscent of the decrease of laminin-1 expression, as a consequence of perturbed myoepithelial architecture. Hence, this suggests that loss of miR-145 expression is an early event during breast cancer progression, which may be valuable as an early detection biomarker or a target for therapy. On the other hand, we observed a trend of association between high miR-205 expression and a favorable clinical outcome in $ER^-PR^-HER2^-$ cases, although in a limited sample of 20 cases. A given patient case can be ascribed to the aggressive basal subtype based on specific gene expression profile, negative status of ER/PR/HER2, and/or expression of basal epithelial cytokeratins (cytokeratin 5/6 and CK14) and other molecular markers, such as EGF receptor (EGFR) and nestin (21, 23, 43). However, it seems that at least two groups exist among basal tumors with distinct courses of the disease and outcome (42, 46), which are not readily discernible based on differential expression of current markers. Thus, miR-205 may have a potential application as an ancillary prognostic indicator of the basal tumor subtype.

A limitation to identifying and validating potential biomarkers is the difficulty of conducting retrospective studies with archived tumor specimens (47) due in part to protein and RNA degradation. Hence, the very small size of miRNAs offers a unique advantage because short RNA molecules are substantially less susceptible than mRNAs to enzymatic and mechanical degradation. Here, we implemented a method for detection of miRNAs in breast cancer specimens, LNA-ISH, which offers a spatial resolution of miRNA expression unsurpassed by other available techniques. Our data show that miRNAs can be detected by ISH in archived FFPE specimens and can be used to obtain clinically relevant information. However, we noticed that long fixation periods in 10% formalin (more than 12–18 h) can affect negatively the intensity of the miRNA *in situ* signal. Some specimens included in our studies were prepared before the implementation of institutional standardization of the formalin fixation and paraffin-embedding protocol. Although this should not affect conclusions comparing matched normal/tumor specimens, the magnitude of changes in miRNA expression observed in some patient cases may reflect more this experimental variation rather than a biological effect. Therefore, comparisons across tumor specimens should be interpreted with caution.

The spatial miRNA expression patterns described in this study should constitute the basis for further retrospective and prospective ISH studies in larger cohorts of breast cancer cases, which will be necessary to validate the robustness and assess the utility of this miRNA signature. Similar ISH studies could be designed to examine already-identified miRNA signatures associated with other types of cancer. We envision that our or similar ISH approaches could be readily adapted in routine clinical practice for assessment of patient cases.

Acknowledgments

Received 8/18/2007; revised 9/19/2007; accepted 10/6/2007.

Grant support: Susan G. Komen Breast Cancer Foundation postdoctoral fellowship (PDF0503563) and Hitchcock Foundation intramural grant (L.F. Sempere); U.S. Army Breast Cancer Research Program grant DAMD17-03-1-2002, Elsa U. Pardee Foundation, and Prouty intramural grant (C.N. Cole); and Danish National Advanced Technology Foundation and Danish Medical Research Council (S. Kauppinen). Wilhelm Johannsen Centre for Functional Genome Research was established by the Danish National Research Foundation.

The costs of publication of this article were defrayed in part by the payment of page charges. This article must therefore be hereby marked *advertisement* in accordance with 18 U.S.C. Section 1734 solely to indicate this fact.

We thank Dr. Victor Ambros in whose laboratory L.F. Sempere started this project and for providing us with miRNA StarFire probes; Drs. Brad Arrick and Ethan Dmitrovsky for use of their tissue culture facilities; Drs. Brad Arrick, Susan Conzen, James DiRenzo, and Alan Eastman for providing us with cell lines; Dr. Susan Holbeck for sending us frozen pellets of the NCI-60 cell panel; Maudine Waterman for her skillful assistance on immunohistochemical assays and creation of the TMA; and members of the authors' laboratories as well as Elena Bryleva, Dr. James DiRenzo, Dr. Ethan Dmitrovsky, Dorrit Nolting, and two anonymous reviewers for support and comments on this manuscript.

References

1. Ambros V. The functions of animal microRNAs. Nature 2004;431:350–5.
2. Bartel DP, Chen CZ. Micromanagers of gene expression: the potentially widespread influence of metazoan microRNAs. Nat Rev Genet 2004;5:396–400.
3. Kloosterman WP, Plasterk RH. The diverse functions of microRNAs in animal development and disease. Dev Cell 2006;11:441–50.
4. Zeng Y. Principles of micro-RNA production and maturation. Oncogene 2006;25:6156–62.
5. Valencia-Sanchez MA, Liu J, Hannon GJ, Parker R. Control of translation and mRNA degradation by miRNAs and siRNAs. Genes Dev 2006;20:515–24.

6. Bentwich I, Avniel A, Karov Y, et al. Identification of hundreds of conserved and nonconserved human microRNAs. Nat Genet 2005;37:766–70.
7. Berezikov E, van TG, Verheul M, et al. Many novel mammalian microRNA candidates identified by extensive cloning and RAKE analysis. Genome Res 2006;16: 1289–98.
8. Didiano D, Hobert O. Perfect seed pairing is not a generally reliable predictor for miRNA-target interactions. Nat Struct Mol Biol 2006;13:849–51.
9. Lewis BP, Burge CB, Bartel DP. Conserved seed pairing, often flanked by adenosines, indicates that thousands of human genes are microRNA targets. Cell 2005;120:15–20.
10. Zhang B, Pan X, Cobb GP, Anderson TA. microRNAs as oncogenes and tumor suppressors. Dev Biol 2007;302: 1–12.
11. Calin GA, Croce CM. MicroRNA signatures in human cancers. Nat Rev Cancer 2006;6:857–66.
12. Calin GA, Dumitru CD, Shimizu M, et al. Frequent deletions and down-regulation of micro-RNA genes miR15 and miR16 at 13q14 in chronic lymphocytic leukemia. Proc Natl Acad Sci U S A 2002;99:15524–9.
13. Calin GA, Ferracin M, Cimmino A, et al. A microRNA signature associated with prognosis and progression in chronic lymphocytic leukemia. N Engl J Med 2005;353: 1793–801.
14. Michael MZ, O' Connor SM, Holst Pellekaan NG, Young GP, James RJ. Reduced accumulation of specific microRNAs in colorectal neoplasia. Mol Cancer Res 2003;1:882–91.
15. Yanaihara N, Caplen N, Bowman E, et al. Unique microRNA molecular profiles in lung cancer diagnosis and prognosis. Cancer Cell 2006;9:189–98.
16. Volinia S, Calin GA, Liu CG, et al. A microRNA expression signature of human solid tumors defines cancer gene targets. Proc Natl Acad Sci U S A 2006;103: 2257–61.
17. Lu J, Getz G, Miska EA, et al. MicroRNA expression profiles classify human cancers. Nature 2005;435:834–8.
18. He L, Thomson JM, Hemann MT, et al. A microRNA polycistron as a potential human oncogene. Nature 2005;435:828–33.
19. Cimmino A, Calin GA, Fabbri M, et al. miR-15 and miR-16 induce apoptosis by targeting BCL2. Proc Natl Acad Sci U S A 2005;102:13944–9.
20. Johnson SM, Grosshans H, Shingara J, et al. RAS is regulated by the let-7 microRNA family. Cell 2005;120: 635–47.
21. Sorlie T. Molecular portraits of breast cancer: tumour subtypes as distinct disease entities. Eur J Cancer 2004;40:2667–75.
22. Sims AH, Ong KR, Clarke RB, Howell A. High-throughput genomic technology in research and clinical management of breast cancer. Exploiting the potential of gene expression profiling: is it ready for the clinic? Breast Cancer Res 2006;8:214.
23. Carey LA, Perou CM, Livasy CA, et al. Race, breast cancer subtypes, and survival in the Carolina Breast Cancer Study. JAMA 2006;295:2492–502.
24. Carey LA, Dees EC, Sawyer L, et al. The triple negative paradox: primary tumor chemosensitivity of breast cancer subtypes. Clin Cancer Res 2007;13: 2329–34.
25. Bertheau P, Turpin E, Rickman DS, et al. Exquisite sensitivity of TP53 mutant and basal breast cancers to a dose-dense epirubicin-cyclophosphamide regimen. PLoS Med 2007;4:e90.
26. Kauppinen S, Vester B, Wengel J. Locked nucleic acid: high-affinity targeting of complementary RNA for RNomics. Handb Exp Pharmacol 2006;173:405–22.
27. Koshkin AA, Wengel J. Synthesis of novel 2′,3′-linked bicyclic thymine ribonucleosides. J Org Chem 1998;63: 2778–81.
28. Castoldi M, Schmidt S, Benes V, et al. A sensitive array for microRNA expression profiling (miChip) based on locked nucleic acids (LNA). RNA 2006;12:913–20.
29. Cole K, Truong V, Barone D, McGall G. Direct labeling of RNA with multiple biotins allows sensitive expression profiling of acute leukemia class predictor genes. Nucleic Acids Res 2004;32:e86.
30. Wienholds E, Kloosterman WP, Miska E, et al. MicroRNA expression in zebrafish embryonic development. Science 2005;309:310–1.
31. Saeed AI, Sharov V, White J, et al. TM4: a free, open-source system for microarray data management and analysis. Biotechniques 2003;34:374–8.
32. Huber W, von HA, Sultmann H, Poustka A, Vingron M. Variance stabilization applied to microarray data calibration and to the quantification of differential expression. Bioinformatics 2002;18 Suppl 1:S96–104.
33. Sempere LF, Freemantle S, Pitha-Rowe I, Moss E, Dmitrovsky E, Ambros V. Expression profiling of mammalian microRNAs uncovers a subset of brain-expressed microRNAs with possible roles in murine and human neuronal differentiation. Genome Biol 2004;5:R13.
34. Griffiths-Jones S, Grocock RJ, van DS, Bateman A, Enright AJ. miRBase: microRNA sequences, targets and gene nomenclature. Nucleic Acids Res 2006;34:D140–4.
35. Neve RM, Chin K, Fridlyand J, et al. A collection of breast cancer cell lines for the study of functionally distinct cancer subtypes. Cancer Cell 2006;10:515–27.
36. Charafe-Jauffret E, Ginestier C, Monville F, et al. Gene expression profiling of breast cell lines identifies potential new basal markers. Oncogene 2006;25: 2273–84.
37. Kloosterman WP, Wienholds E, de BE, Kauppinen S, Plasterk RH. *In situ* detection of miRNAs in animal embryos using LNA-modified oligonucleotide probes. Nat Methods 2006;3:27–9.
38. Nelson PT, Baldwin DA, Kloosterman WP, Kauppinen S, Plasterk RH, Mourelatos Z. RAKE and LNA-ISH reveal microRNA expression and localization in archival human brain. RNA 2006;12:187–91.
39. van Gijlswijk RP, Wiegant J, Vervenne R, Lasan R, Tanke HJ, Raap AK. Horseradish peroxidase-labeled oligonucleotides and fluorescent tyramides for rapid detection of chromosome-specific repeat sequences. Cytogenet Cell Genet 1996;75:258–62.
40. Iorio MV, Ferracin M, Liu CG, et al. MicroRNA gene expression deregulation in human breast cancer. Cancer Res 2005;65:7065–70.
41. Hwang HW, Wentzel EA, Mendell JT. A hexanucleotide element directs microRNA nuclear import. Science 2007;315:97–100.
42. Clarke C, Sandle J, Lakhani SR. Myoepithelial cells: pathology, cell separation and markers of myoepithelial differentiation. J Mammary Gland Biol Neoplasia 2005; 10:273–80.
43. Li H, Cherukuri P, Li N, et al. Nestin is expressed in the basal/myoepithelial layer of the mammary gland and is a selective marker of basal epithelial breast tumors. Cancer Res 2007;67:501–10.
44. Laakso M, Loman N, Borg A, Isola J. Cytokeratin 5/14-positive breast cancer: true basal phenotype confined to BRCA1 tumors. Mod Pathol 2005;18:1321–8.
45. Zhan M, Miller CP, Papayannopoulou T, Stamatoyannopoulos G, Song CZ. MicroRNA expression dynamics during murine and human erythroid differentiation. Exp Hematol 2007;35:1015–25.
46. Sotiriou C, Neo SY, McShane LM, et al. Breast cancer classification and prognosis based on gene expression profiles from a population-based study. Proc Natl Acad Sci U S A 2003;100:10393–8.
47. Ludwig JA, Weinstein JN. Biomarkers in cancer staging, prognosis and treatment selection. Nat Rev Cancer 2005;5:845–56.
48. Rae JM, Ramus SJ, Waltham M, et al. Common origins of MDA-MB-435 cells from various sources with those shown to have melanoma properties. Clin Exp Metastasis 2004;21:543–52.
49. Liscovitch M, Ravid D. A case study in misidentification of cancer cell lines: MCF-7/AdrR cells (re-designated NCI/ADR-RES) are derived from OVCAR-8 human ovarian carcinoma cells. Cancer Lett 2007;245: 350–2.

Altered MicroRNA Expression Confined to Specific Epithelial Cell Subpopulations in Breast Cancer

Lorenzo F. Sempere, Mette Christensen, Asli Silahtaroglu, et al.

Cancer Res 2007;67:11612-11620.